Nuclear Inst. and Methods in Physics Research, A 940 (2019) 61–65

Contents lists available at ScienceDirect

Nuclear Inst. and Methods in Physics Research, A

journal homepage: www.elsevier.com/locate/nima

Influence of the RF magnetic field on beam dynamics in SC200 cyclotron

G. Karamysheva [a,*], D. Popov [a], O. Karamyshev [a], V. Malinin [a], T. Karamysheva [a,c], G. Shirkov [a], S. Shirkov [a], Y. Bi [b], G. Chen [b], W. Chuansong [b], K. Ding [b], Y. Song [b]

[a] Joint Institute for Nuclear Research, Dubna, Russia
[b] Institute of Plasma Physics, Chinese Academy of Sciences, Hefei, China
[c] Federal Research Center "Computer Science and Control" of the Russian Academy of Sciences, Moscow, Russia

ARTICLE INFO

Keywords:
Cyclotron accelerating system
Beam dynamics
Phase expansion/compression effect

ABSTRACT

The SC200 superconducting cyclotron is developed by the collaboration between ASIPP (Hefei, China) and JINR (Dubna, Russia). The SC200 cyclotron will deliver 200 MeV beam for proton therapy and research.

The influence of the time-dependent magnetic field created by the acceleration system of SC200 should be taken into account in beam dynamics simulations and during the shimming procedure, as two conditions are present together: first — due to the spiral shape of the accelerating cavities, there is no vertical plane of symmetry through the middle of the dee; and second — second harmonic mode of acceleration in four-sector magnet structure imposes that the RF phase shift from beam entrance of the dee to its exit is not 180 degrees.

Particle tracking was performed with 3D maps of electromagnetic fields obtained from computer modelling of the magnet system and the accelerating RF cavities using CST Studio Suite. We have calculated particle dynamics taking into account RF magnetic field and have estimated a value of additional mean field needed for the compensation of beam phase lag induced by RF magnetic field. And finally, we designed a shim that should form the required additional field.

1. Introduction

SC200 is an isochronous superconducting compact cyclotron [1]. Superconducting coils will be enclosed in a cryostat, all other parts are warm. Internal ion source of PIG type will be used. For proton acceleration we are planning to use two accelerating RF cavities (Fig. 1) placed in the valleys, operating in the second harmonic mode. RF system will operate at the frequency of 91.5 MHz. Magnet of the cyclotron has a four-sector structure. Mean magnetic field of the cyclotron will be in the range of 2.9T–3.5T (centre-extraction).

2. The electro-magnetic field from RF-cavity simulation

The model of the RF cavities was simulated in CST MICROWAVE STUDIO [2] with eigenmode JD loss-free solver (Jacobi Division Method) and 20 M hexahedral mesh. Voltage on the first and second gaps was calculated separately and can be seen in Fig. 2.

Power dissipation in the model was calculated assuming the wall material is copper with a conductivity of $5.8 \cdot 10^7$ S/m. The quality factor was about 6400 and power losses of the model were about 64 kW (peak) for 70 kV voltage in the centre.

The surface currents on the edges of a dee (Fig. 3) caused by the non-zero voltage derivatives (of Fig. 2) produce time-dependent magnetic field perpendicular to the median plane (Fig. 4). As you can see at the radii where dU/dR equals zero, B_z equals zero as well.

The map of the amplitude of the time dependent magnetic field (B_{rf}), generated in the RF cavities was obtained and analysed as well. From Figs. 5 and 6 one can see that the magnetic field induced by RF system (at time when E=0, RF phase=90°) has different signs in two accelerating gaps of each cavity everywhere except for the areas near the stems: at R=40 cm. At the radii close to the stems there is no compensation of magnetic field in two gaps.

3. Beam dynamic simulation

We also simulated beam dynamics with the calculated fields: 3D magnetic field map and 3D electric field map from RF cavity simulation were used. We used CST Studio for simulation of the magnet system and for creation of the 3D magnetic field map. Firstly, simulations were performed for central particle. Accurate simulation of the influence of the RF magnetic field revealed a big slip of the phase of the accelerated particle — up to 20° RF at R ∼ 40 cm. We plot in Fig. 7 the positions

* Corresponding author.
E-mail addresses: gkaram@jinr.ru (G. Karamysheva), podivs@jinr.ru (D. Popov).

https://doi.org/10.1016/j.nima.2019.05.066
Received 30 January 2019; Received in revised form 6 May 2019; Accepted 21 May 2019
Available online 3 June 2019
0168-9002/

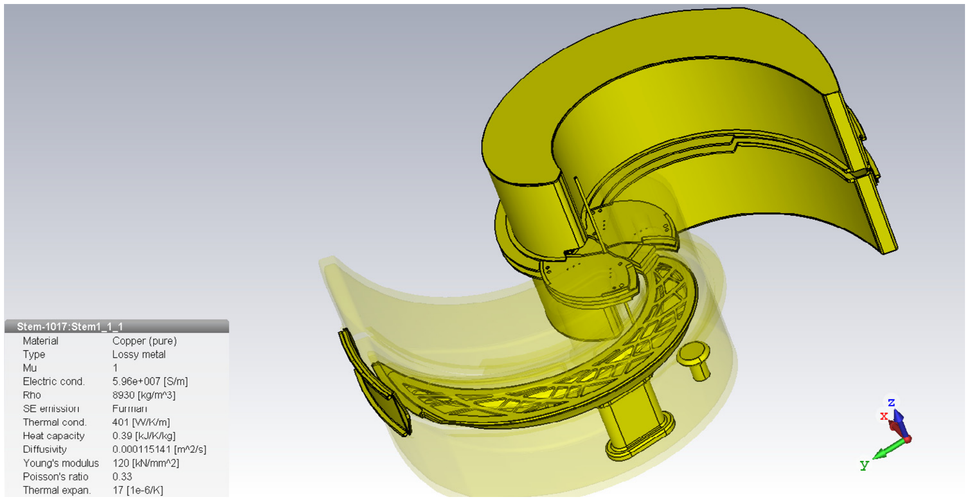

Fig. 1. The model of RF Cavity.

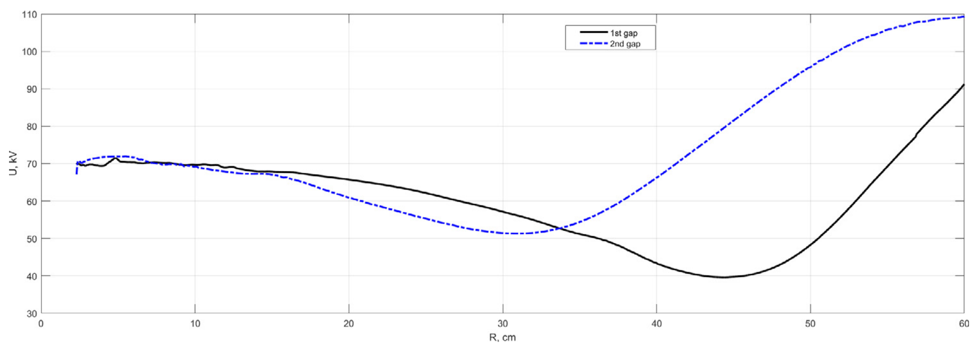

Fig. 2. Voltage distribution of accelerating gaps along radius.

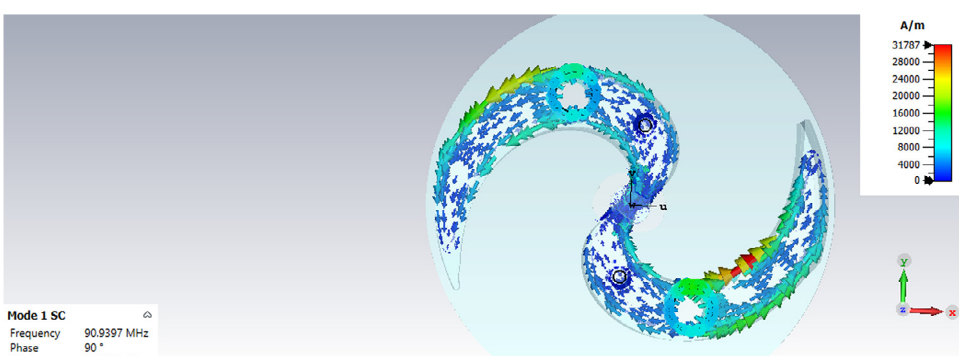

Fig. 3. Surface currents inside RF-cavity.

of the reference particle at the moment when the electric field is zero. The particle moves counterclockwise, and the RF time dependent magnetic field causes the phase lag of the particle. The similar effect was observed in superconducting cyclotron ACCEL [3]. It should be compensated during the shimming procedure otherwise it will lead to additional particle losses in extraction.

4. Compensation of B_{rf} action and phase compression effect

Because of the action of the time-dependent RF magnetic field induced by accelerating cavity the mean field isochronous on equilibrium orbits should be changed to compensate action of the B_{rf}. For ideally isochronous magnetic field the value of the compensation field can be estimated from a simple formula:

$$B_{add} = -B_{rf\,mean} \cdot cos(h \cdot \theta_{cav}/2),$$

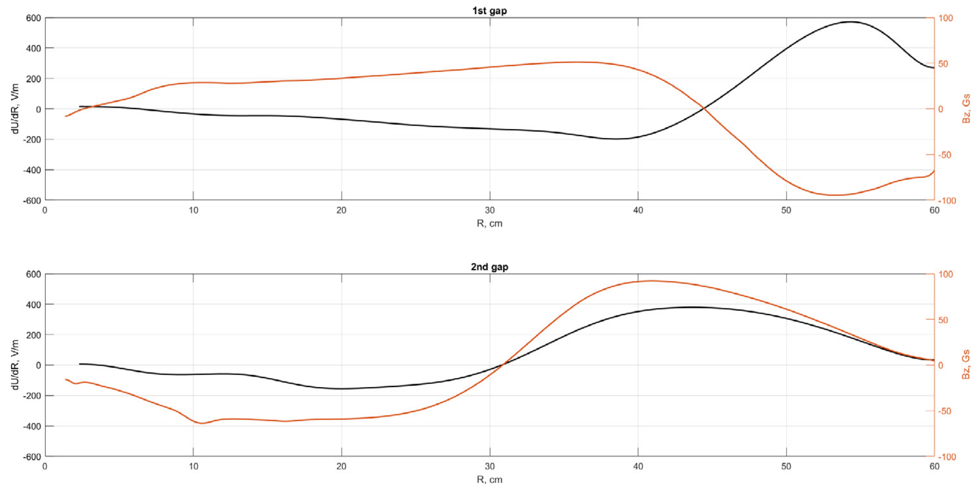

Fig. 4. Radial derivatives of accelerating gaps' voltage (black), value of magnetic field in gaps' centres generated by that derivatives (grey), all with respect radius.

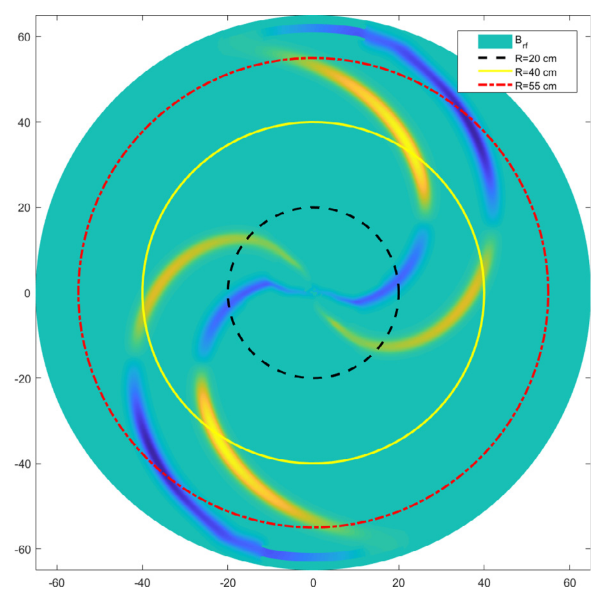

Fig. 5. Magnetic field generated by the acceleration system. Dashed, solid and dotdash circles mark locations of data presented in the next figure.

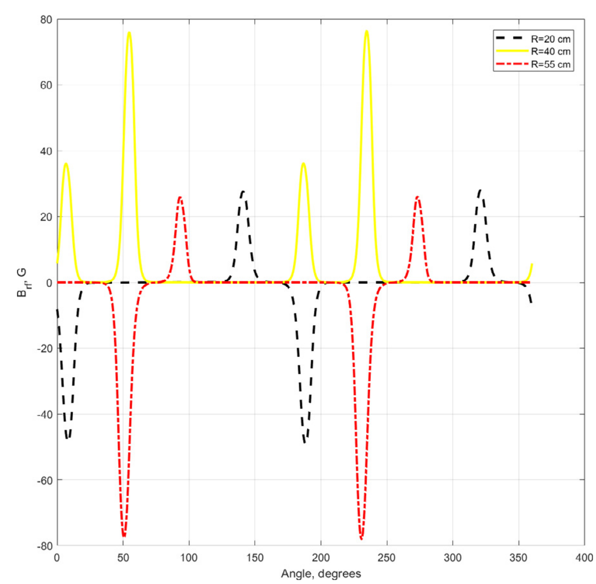

Fig. 6. Magnitude of the magnetic field generated by the acceleration system for different radii versus azimuthal angle.

where θ_{cav} — azimuthal extension of the cavity (see Fig. 8), h — harmonic number. The value of the RF magnetic field, when the RF phase=90°, averaged over azimuth angle - $B_{rf\,mean}$ is presented in Fig. 13. The additional field B_{add} calculated by this formula is also shown in the figure. Particle tracking simulation was also conducted with compensated field and the compensation was proved to be correct (Fig. 9).

This phase lag effect due to the mean magnetic field of the RF cavity arises only if the harmonic used for acceleration does not correspond exactly to the width of the accelerating cavities. In our case, the azimuthal extension of the cavities is about 45° (see Fig. 8), which is optimal for the 4th harmonic of the acceleration, but not for the second harmonic used in our cyclotron. We simulated an artificial situation with 4th harmonic acceleration with RF frequency of 91.5 × 2 MHz in the same magnet field maps. The simulation results can be seen in Fig. 10. The phase lag of particles is absent.

As the voltage along radius is increasing substantially (about twice) in the radii from 40 to 60 cm (see Fig. 2) we should observe phase compression effect which is visible in Fig. 10 at R>50. The phase compression–phase expansion effect was firstly mentioned by Mueller and Mahrt [4].

As for SC200 model, phase compression is observed disregarding the mean field compensation (as it should be). In Fig. 11 phase width of the bunch for the simulation taking into account time-dependent RF magnetic field and its compensation (black lines) is smaller at the end of acceleration than without taking them into account.

5. The implementation of B_{rf} compensation

After testing of numerous variety of models we came to the conclusion that the optimal shim would be parallel to the tangent to the surface of the sector at R=40 cm, placed 11 cm above the median plane and approximately 3 mm thick (Fig. 12). Being placed on every sector

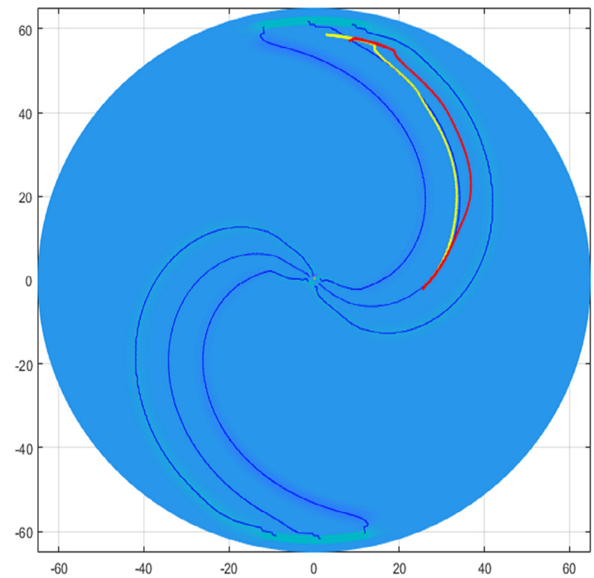

Fig. 7. Central particle positions: white line — no B_{rf}, deviated black line — with B_{rf}, both at the moment when RF phase is equal zero. Other grey lines indicate maximums of electric field distribution and middles of the cavities.

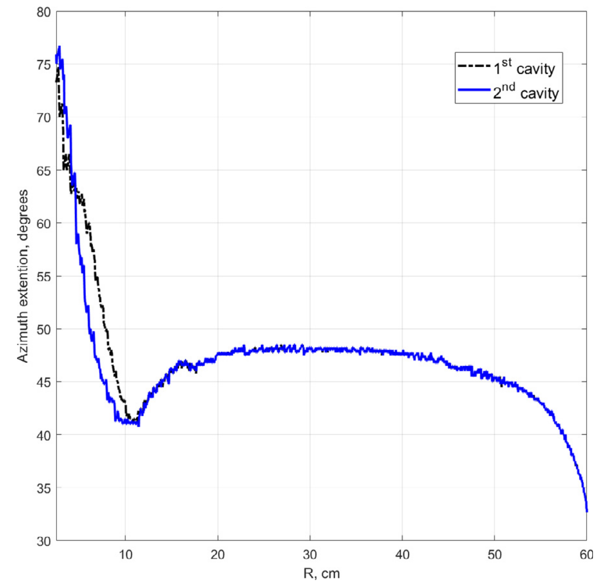

Fig. 8. Azimuthal extension of the cavity (between the maximums of the field distribution).

it produces the field that provides the necessary compensation with accuracy better then 1 Gs (Fig. 13), which is quite enough.

6. Conclusion

In our simulations we faced two different effects of the time-dependent RF magnetic field on the particle motion. The first one is a phase lag of the particles. This effect is induced by uncompensated RF magnetic field in two gaps, caused by its asymmetric distribution in that gaps (Figs. 4, 5, 6), and cavity width smaller the 180 RF degrees. This phase lag is big enough and can be compensated by increase of the mean magnetic field. The second one is a phase compression effect which occurs due to the change of voltage along the gap. This effect leads, in our case, to phase compression, so it is good for extraction.

Compensation of the RF magnetic field was simulated. It required a full cycle of working iterations: assessing the impact, beam dynamic simulation and correction phase. As the result after compensation we obtained the mean magnetic field isochronous for particles influenced by the RF magnetic field.

Acknowledgement

We are grateful to L. Calabretta for fruitful discussion and interesting ideas.

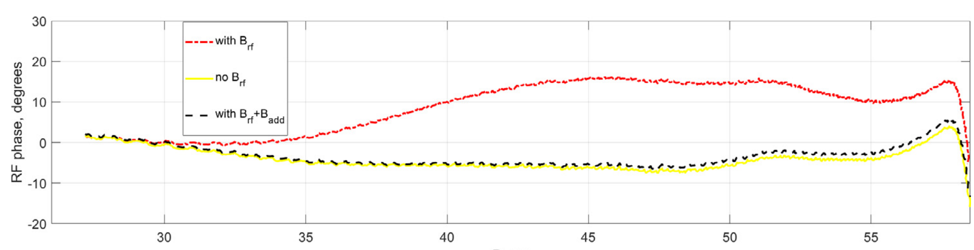

Fig. 9. Phase motion of the central particle neglecting B_{rf} (solid line), taking into account RF magnetic field (dotdash line) and with $B_{rf}+B_{add}$ (dashed line). Positive phase corresponds to the lagging particle.

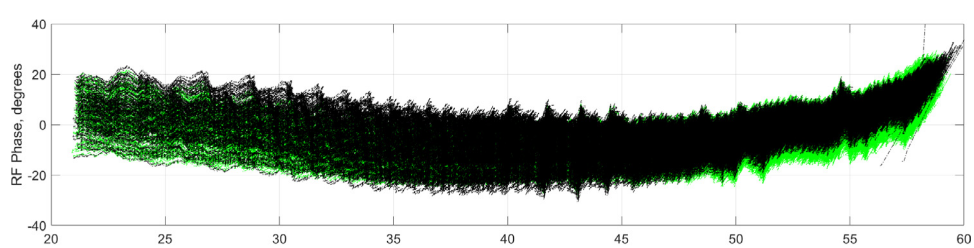

Fig. 10. Phase motion of the beam without RF magnetic field (grey lines) and phase motion with RF magnetic field but without compensation field (black lines). Accelerated with the RF frequency of 91.5 × 2 MHz.

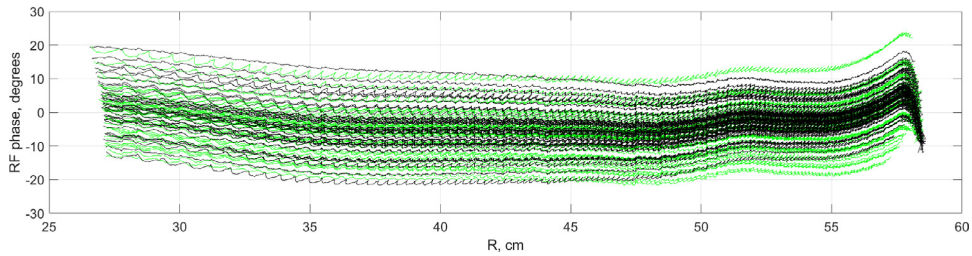

Fig. 11. Phase motion of the beam without RF magnetic field (grey lines) and phase motion with RF magnetic field and compensation field (black lines).

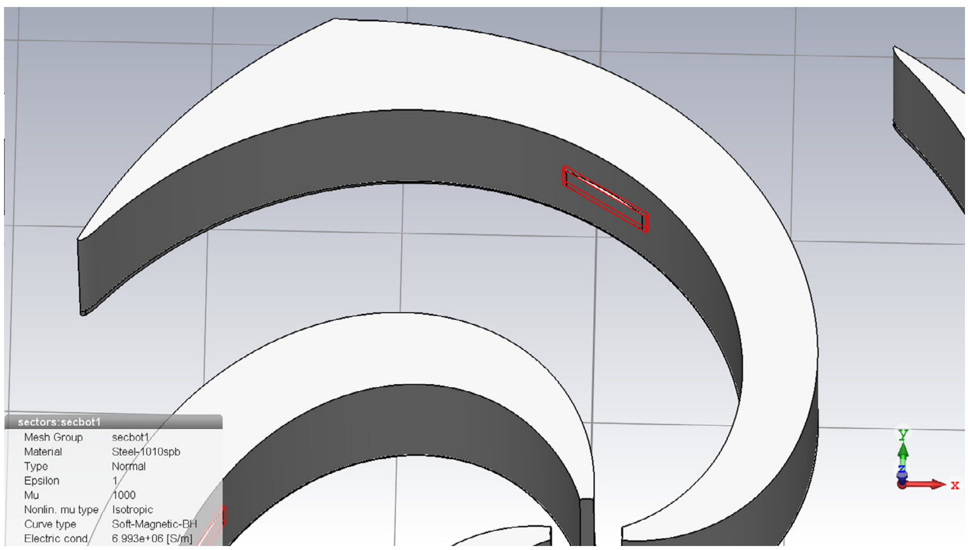

Fig. 12. The location and the shape of the shim inserted into a sector.

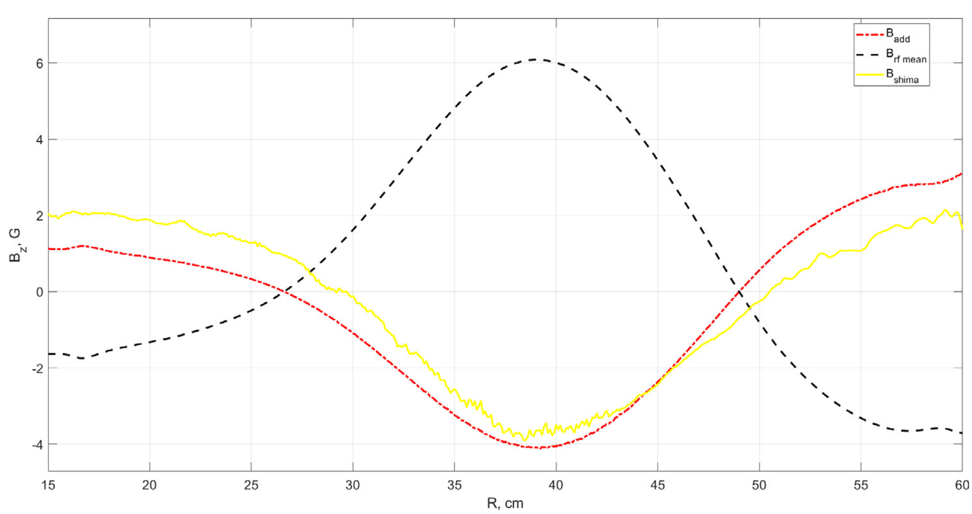

Fig. 13. Mean value of B_{rf} field (dashed line), additional field (dotdash line) and the implementation of additional field with the shim (solid line), all versus radius.

References

[1] G. Karamysheva, et al., Present status of the SC202 superconducting cyclotron project, in: VIIIth International Particle Accelerator Conference (IPAC 2017), Copenhagen, Denmark, THPVA120.

[2] CST Studio Suite. https://www.cst.com/.

[3] J.M. Schippers, et al., Beam-dynamics studies in a 250 MeV superconducting cyclotron with a particle tracking program, Nukleonika 48 (Supplement 2) (2003) S145–S147.

[4] R.W. Mueller, R.W. Mahrt, Nucl. Inst. Meth. 86 (1970) 241.